UNIVERSITY OF WASHINGTON

DEPARTMENT OF OCEANOGRAPHY

Technical Reports

Nos. 200, 201, 202, 203, 204, and 205

A COMPILATION OF ARTICLES REPORTING RESEARCH

SPONSORED JOINTLY BY

THE U.S. ATOMIC ENERGY COMMISSION

and

THE OFFICE OF NAVAL RESEARCH

U.S. Atomic Energy Commission
Contract AT(45-1)-1725
and
Office of Naval Research
Contracts Nonr -477(37)
and Nonr-477(10)
Project NR 083 012

Reference M67-52
September 1967

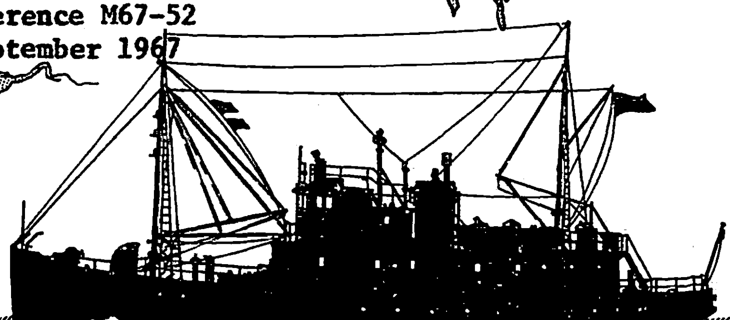

SEATTLE, WASHINGTON 98105

UNIVERSITY OF WASHINGTON
DEPARTMENT OF OCEANOGRAPHY
Seattle, Washington 98105

Technical Reports

Nos. 200, 201, 202,
203, 204, and 205

A COMPILATION OF ARTICLES REPORTING RESEARCH SPONSORED JOINTLY BY THE U.S. ATOMIC ENERGY COMMISSION and THE OFFICE OF NAVAL RESEARCH

U.S. Atomic Energy Commission
Contract AT(45-1)-1725
and
Office of Naval Research
Contracts Nonr-477(37)
and Nonr-477(10)

Richard H. Fleming
RICHARD H. FLEMING
Chairman

Clifford A. Barnes
CLIFFORD A. BARNES
Principal Investigator

ARTICLES REPORTING RESEARCH SPONSORED JOINTLY BY THE U.S. ATOMIC ENERGY COMMISSION AND THE OFFICE OF NAVAL RESEARCH

Technical Report No. 200

NOTES ON PATAGIUM IN THE RADIOLARIAN GENERA HYMENIASTRUM AND DICTYASTRUM, by Hsin-Yi Ling. Micropaleontology, *12*(4): 489–492. 1966.

Technical Report No. 201

PHYSIOGRAPHY OF COBB AND GORDA RISES, NORTHEAST PACIFIC OCEAN, by Dean A. McManus. Geological Society of America Bulletin, *78*:527–546. 1967.

Technical Report No. 202

ORGANIC CARBON IN SURFACE SEDIMENT FROM THE NORTHEAST PACIFIC OCEAN, by M. Grant Gross. International Journal of Oceanology and Limnology, *1*(1): 46–54. 1967.

Technical Report No. 203

CURRENTS AT THE COLUMBIA RIVER MOUTH, by Alyn C. Duxbury. Photogrammetric Engineering, *33*(3):305–310. 1967.

Technical Report No. 204

SEDIMENT MOVEMENT ON THE CONTINENTAL SHELF NEAR WASHINGTON AND OREGON, by M. Grant Gross and Jack L. Nelson. Science, *154*(3750):879–885. 1966.

Technical Report No. 205

TIDAL PERIOD OSCILLATIONS OF AN ISOHALINE SURFACE OFF THE MOUTH OF THE COLUMBIA RIVER, by Alyn C. Duxbury and Noel B. McGary. International Journal of Oceanology and Limnology, *1*(2):71–84. 1967.

Tidal Period Oscillations of an Isohaline Surface Off the Mouth of the Columbia River[1]

Alyn C. Duxbury

Noel B. McGary

Department of Oceanography, University of Washington, Seattle

ABSTRACT *Near the mouth of the Columbia River the river effluent forms a surface pool of low salinity water having distinct boundaries. The periodic motion of this pool and the magnitude of the accompanying changes in water characteristics have made it difficult to obtain directly quasi-synoptic measurements. To interpret these changes in both time and space, a repetitive series of observations was made, and depth-time profiles were interpolated for various parameters at selected points within this area of dilution. Vertical oscillations of equiscalar surfaces were found to be correlated with tidal periodicity. The variation in slope of the equiscalar surfaces with time along a three-station line was used in determining the motion of the periphery of the pool of low salinity surface water past the three stations.*

INTRODUCTION

The effluent from the Columbia River, composed of river water and ebbing tidal flow, enters the coastal water of the Northeast Pacific Ocean and forms a distinct surface pool of low salinity water near the river mouth. The pool moves primarily in response to the tidal forces, hydraulic forces, and surface wind stress. Its presence and motion has been observed on many cruises, but the lack of information on its periodicity and magnitude of displacement has made it difficult to obtain directly synoptic measurements near the river mouth. In order to acquire some insight into the magnitude of the changes occurring in the water structure, a time study of oceanographic conditions was made at a series of stations off the river mouth on *Brown Bear* cruise 351, 15 to 29 September 1964. Repeated observations (approximately 4- to 8-hour intervals) were made at these stations (Fig. 1) over several tidal cycles to determine temporal variations of salinity, temperature, and dissolved oxygen. Two studies were made during the cruise: the first station grid (V, W, X, Y, Z) was sampled during 19 to 22 September and the second (V, M, X, L, U, Y) from 25 to 27 September. The data taken during the first station sequence indicated

[1] Contribution number 409, Department of Oceanography, University of Washington.

Int. J. Oceanol. & Limnol. Vol. 1, No. 2. p. 71-84.

FIGURE 1. Station locations, *Brown Bear* cruise no. 351.

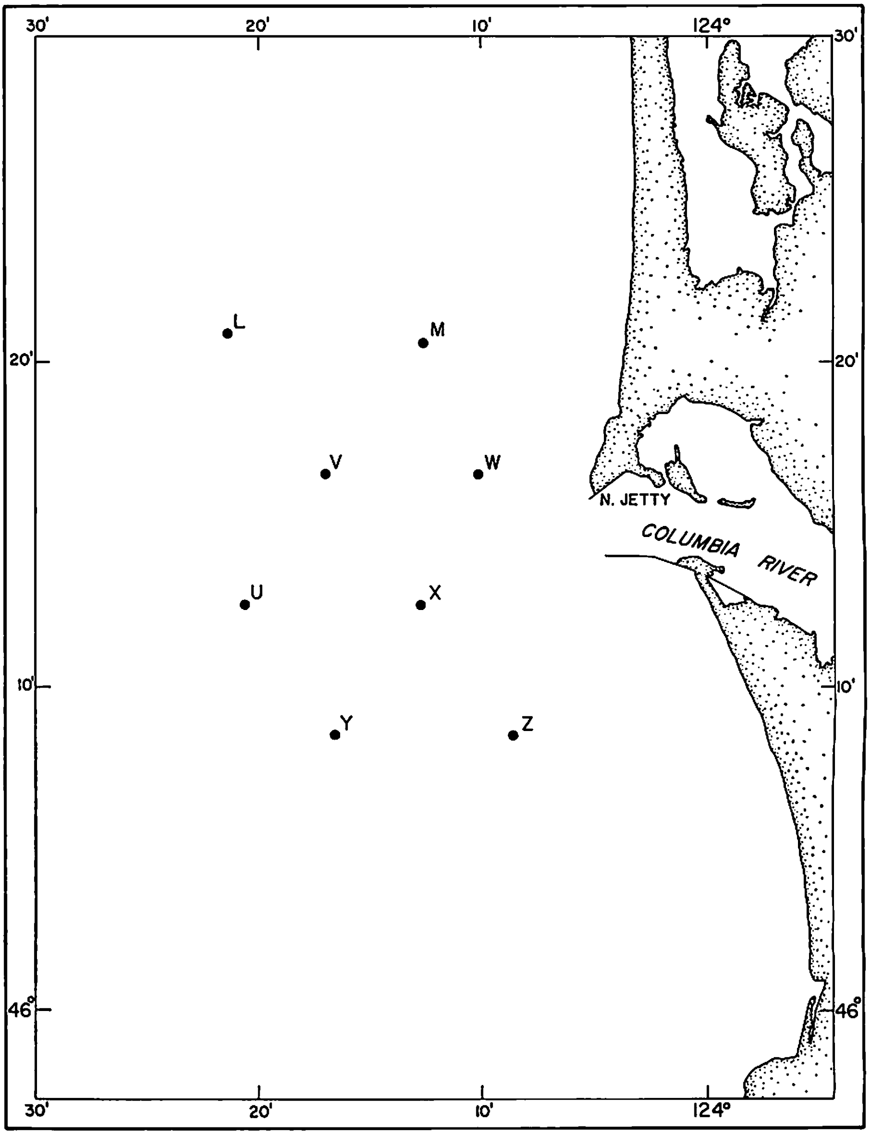

that the core of the low salinity surface water associated with river effluent was north of the five-station grid; this displacement governed the choice of station positions during the second sequence.

Fig. 2 shows the hourly vector winds in the area during the first period. On the 18th and 19th winds blew from the south, switched to northwesterly on the 20th, and continued thus until the midday period on the 21st. A shift to southerly winds then occurred, and these continued until mid-afternoon on the 22nd. The northwesterly winds on the 20th and 21st were apparently of insufficient strength and duration to overcome the effect of the earlier southerly winds on the effluent pool and to drive it south. Consequently the station grid was changed to the V, M, X, L, U, Y, series in an attempt to bracket the low salinity core. However strong northerly winds began as soon as the second series was started and persisted throughout the sampling period. These winds succeeded in moving the surface waters southward. The original five-station sequence showed that despite the first wind shift the core of the low salinity surface water suffered no appreciable net drift, but oscillated about its mean position. Data are presented here in detail to show the oscillatory variations in the water structure due primarily to tide-induced oscillations of this effluent.

FIGURE 2. Hourly wind vectors, speed and direction, 19-22 September in the station area.

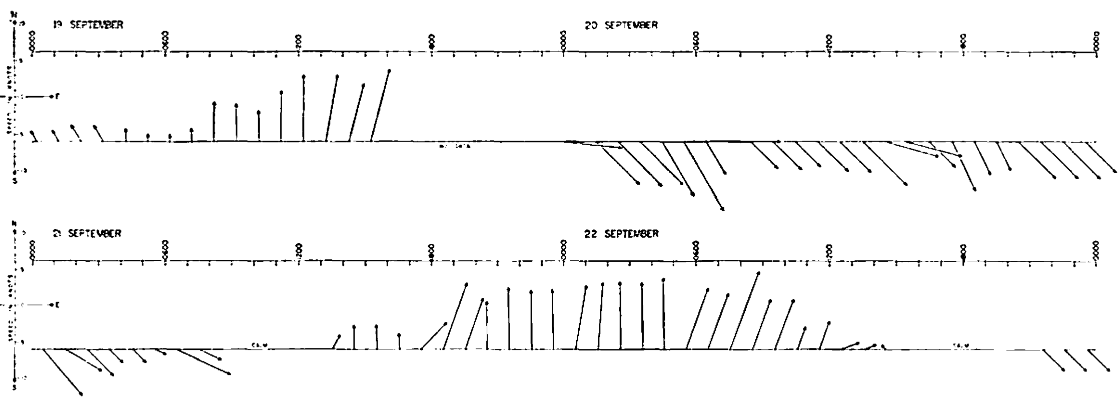

SAMPLING PROCEDURE The key central station X in the first grid (V, W, X, Y, Z) was sampled twice as frequently as the others. Data obtained there were used to guide the construction of time-dependent curves through the data points obtained at the remaining four stations. This use of data from station X is appropriate because it had been occupied as an anchor station for a period of 28 hours prior to the five-station sequence. During the anchor period hourly casts were made, alternately using standard oceanographic casts and an *in situ* conductivity-temperature device. The hourly observations obtained at anchor provided a suitable base of reference for the response of the measured variables in the water column to the tide curve, and were further used as a guide in fitting the curves to the less frequent observations made at station X during the five-station sequence. These adjusted station X data were then used as an aid in curve fitting for the other four stations. Verification of the adjusted curves was obtained when station V was used as the anchor station and studied similarly prior to the second time-study sequence. The interpolated data determined for station V during the earlier five-station sequence were in good agreement with the hourly data obtained while at anchor.

Standard procedures were followed in collecting water samples and measuring *in situ* temperatures at each station. Nansen reversing bottles equipped with reversing thermometers were used to obtain samples at 0, 3, 6, 8, 10, 12, 15, 20, 25, and 30 meters as water depth permitted. The primary variables determined were salinity, temperature, and dissolved oxygen concentration. The samples were analyzed for salinity on shipboard using a conductivity bridge and the dissolved oxygen was determined by titration.

Figs. 3-5 show the vertical variation of salinity, temperature, and dissolved oxygen with time at the five stations for the sampling period (0000 hr 21 September to 0000 hr 23 September). The vertical lines with short cross-ticks indicate the time and position of actual measurements. The shapes of the curves constructed through the data points were obtained by the techniques outlined above.

RESULTS The three variables, salinity, temperature, and dissolved oxygen, reflect vertical oscillations of tidal period with amplitudes many times the tidal amplitude (Figs. 3-5). Depressed salinity is the best indicator of the presence of the river effluent, especially during late summer when the Columbia River accounts for more than 90% of the freshwater added locally by rivers (Budinger, Coachman, and Barnes, 1964). Station W in Fig. 3 shows considerable dilution at the sea surface and a rapid increase in salinity with depth just below the surface; this gradient oscillates in the vertical and increases and decreases with the tidal stage. Station V, also on the north of the grid, shows near-surface dilution at depths comparable to those at W. The vertical oscillation of the salinity gradient at V is similar to that at W, but the temporal increase or decrease in the gradient is less apparent. At V the direct response of the gradients to a local periodic addition of river effluent or to the periodic passing of a distinct boundary seems to be missing. At station X, however, the thickness of diluted seawater layer is less than at either V or W, but the salinity gradient changes markedly in response to the periodic motion of the river effluent. The salinity pattern at X apparently represents the periodic presence or absence of the primary effluent pool. The deeper isopleths of salinity at this station respond significantly to the presence and absence of this surface layer of less saline water. Stations Y and Z, especially Z, respond to the tidal oscillation by a vertical displacement of the gradient due to the periodic overburden of effluent water, but show little or no change in the strength of the gradients. These data indicate that the effect of the river water occurs predominantly at stations W and X and that the core of the effluent was located north of the grid. The small gradients at Z and Y indicate that the seawater there suffers less dilution than that at the other stations. The supply of salt by upwelling in the region of Z can also decrease the apparent surface dilution.

During the late summer, the usual configuration of river effluent is plumelike, beginning near the river mouth and with central axis extending southwest, passing through stations X and Y. This distribution should favor high dilution at X and Y, but a common occurrence in summer is a northward displacement of the river effluent near the river mouth (Budinger et al., 1964).

A pronounced band of upwelled water is usually found between station Z and the coast from late spring to early fall. This is oceanic water from middepths that replaces surface water carried offshore to the southwest by the predominant northerly winds of summer. This upwelled water is relatively uniform with higher salinity, lower temperature, and lower dissolved oxygen content than is normally associated with coastal surface water. Figs. 3-5 show this type water at stations Z and Y. Insolation, photosynthetic processes, and surface mixing create the sharp gradients in temperature and oxygen at the 10- to 12-meter depth in this upwelled water, but have little effect on the salinity structure. Pattulo and Denner (1965) have shown how the thermal structure of upwelled water changes seasonally along the Oregon coast.

The isograms in Fig. 3-5 indicate oscillations of the boundary with tidal period. However, the amplitude of the oscillation and the timing of the crest vary slightly for each of the five stations. These slight variations show in the temporal change in the depth profile of an isopleth across three of the grid stations. Fig. 6 shows the temporal variation of the depth of the $31^0/_{00}$ salinity surface along the two intersecting lines taken through the five stations for the full survey period, whereas Fig. 3-5 are truncated for convenience. The time-distance plots of a constant value surface are interpreted as follows: If the depth contours (1-m depth increments), of the equiscalar surface are parallel to the time axis, the surface is not moving along the station profile line, $dx/dt = 0$, and the slope of this surface, dz/dx, is given by the rate of change of the contour interval along the station line. If the depth contours are inclined to the time axis, the surface is moving along the station line in the direction indicated by the sign of dx/dt. This motion may be a bodily displacement of the surface along the station line (maintaining a constant slope with contours parallel to each other but inclined to the time axis); or it may be a horizontal displacement occurring at different rates with depth causing the slope of the surface to change with time (contours inclined to each other and also

FIGURE 3. Salinity versus depth versus time at the five stations; V, W, X, Y, Z, 21-22 September.

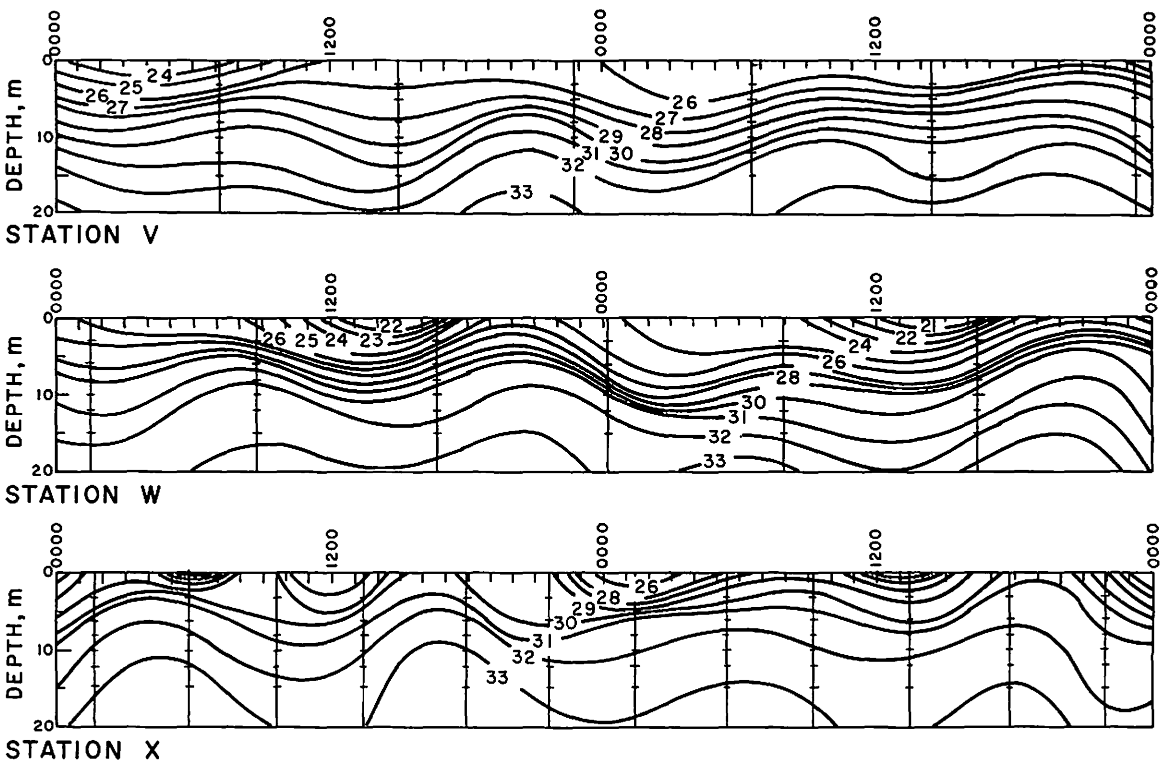

to the time axis). The motion of the surface displayed in Fig. 6 is comparable to traveling oscillations (internal waves). However, the wave-like motion does not exist remote from the center of the station grid. In this respect, the oscillations of the deeper surfaces are localized and are related to the migration of the boundary of the river effluent. The oscillation seems to be purely tidal as the effluent pool moves in response to the ebb and flow in the river estuary. No wind-induced oscillations such as found by Cairns and Lafond (1966) were evident within this limited area at the time studied. Periodic changes in the intensity of mixing at the boundary between the effluent and the deeper water could also make the

FIGURE 3. *Continued*

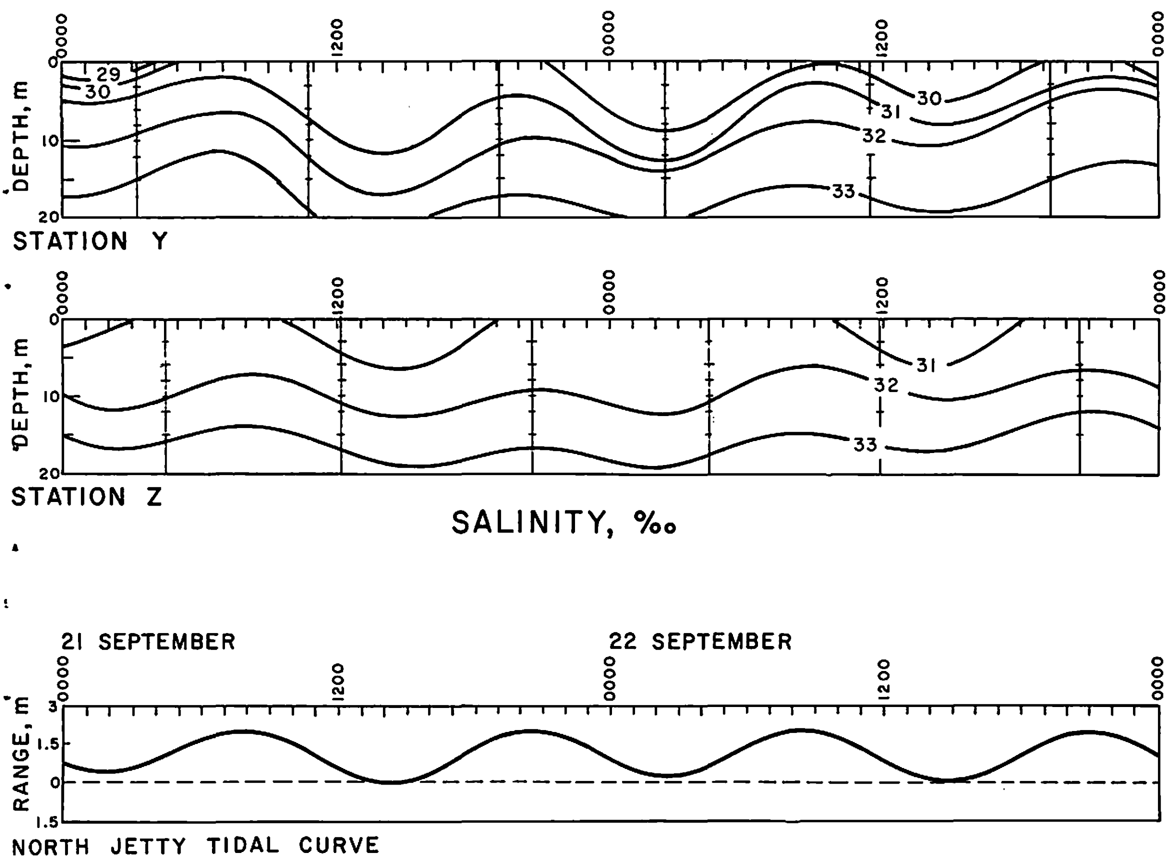

isopleth appear to oscillate in the vertical. However this would also require rapid periodic removal of salt from the surface pool and addition of salt to the lower edge of the boundary. There is no doubt that mixing is extremely important in controlling the distribution of salinity in the area under study. However direct observation of the motion of the lateral boundary as seen at the surface of the effluent indicates to the authors that the migration of this surface pool is more important in producing the oscillations.

The time-space sections are drawn for both the VXZ and the WXY station lines. Motion as determined by dx/dt in Fig. 6 is along VXZ and

FIGURE 4. Temperature versus depth versus time at the five stations; V, W, X, Y, Z, 21-22 September.

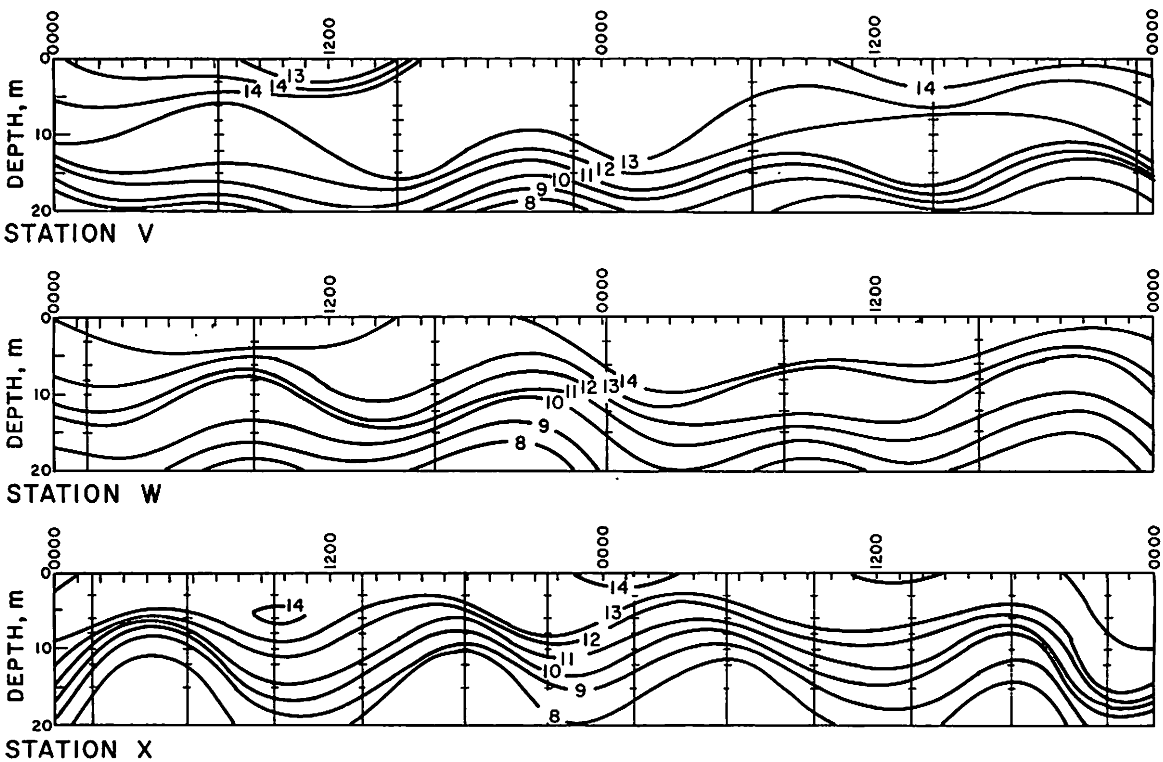

WXY lines, which are neither straight nor perpendicular (Fig. 1). However, the angle between the lines is great enough that components of motion can be calculated along these two lines to give the effective motion across the station grid. The time-dependent displacements of the $31^0/_{00}$ salinity surface along these intersecting lines is shown against the North Jetty tidal curve and the tidal current vectors from Marmer's hodograph at the Columbia River lightship (Marmer, 1926). The hodograph has been adjusted to the time base for the North Jetty tidal curve. In general the surface along the VXZ line is stationary midway between low water and the following high water. The slope of the surface is generally steeper

FIGURE 4. *Continued*

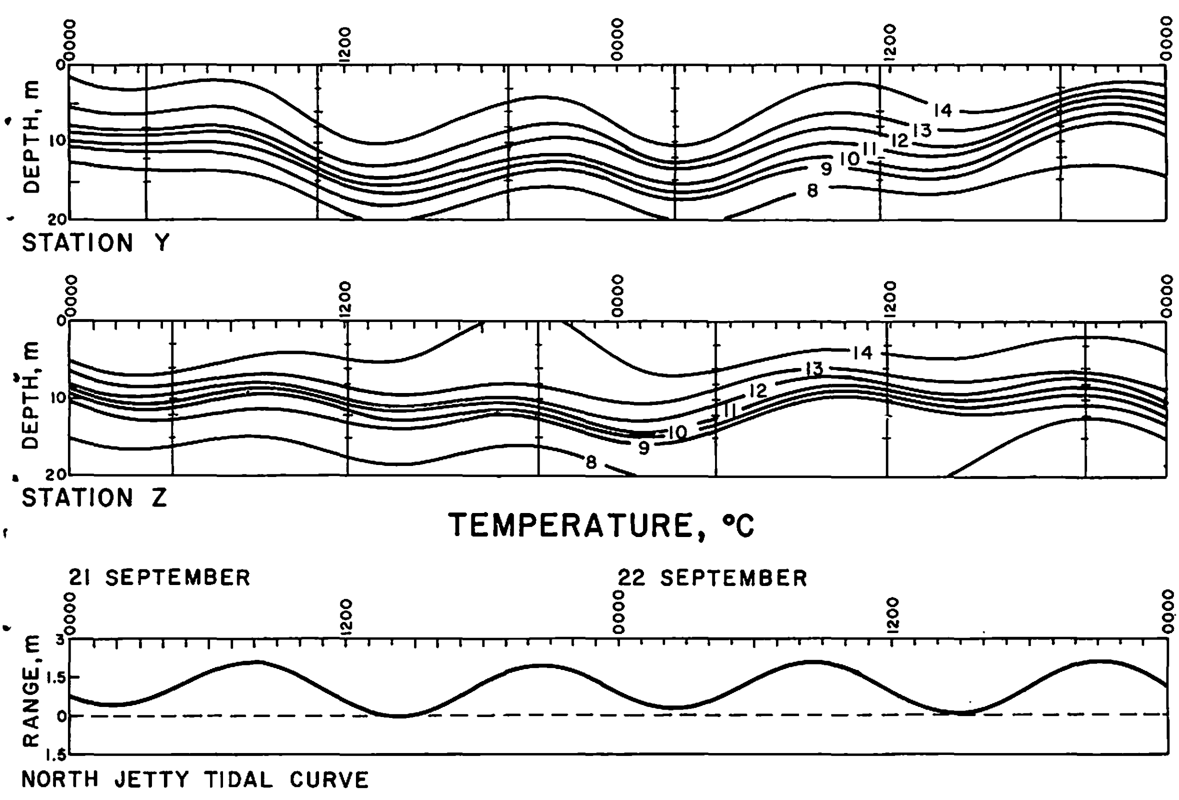

between stations V and X than between X and Z, but occasionally at high water the slope increases between X and Z. Reversals in the slope often appear at low water, causing the isohaline surface to rise toward the sea surface at X and increasing the amplitude of the oscillation. The tilted isohaline surface then moves from V toward Z with the midpoint of the motion period occurring near high water. This motion appears to be uniform and relatively slow (except from 2000 to 2100 hr, 20 September), causing little change from the previously existing slope of the isohaline surface. Prior to low water the motion of this surface toward Z ceases and the slope decreases between X and Z. With the rising tide the slope con-

FIGURE 5. Dissolved oxygen versus depth versus time at the five stations; V, W, X, Y, Z, 21-22 September.

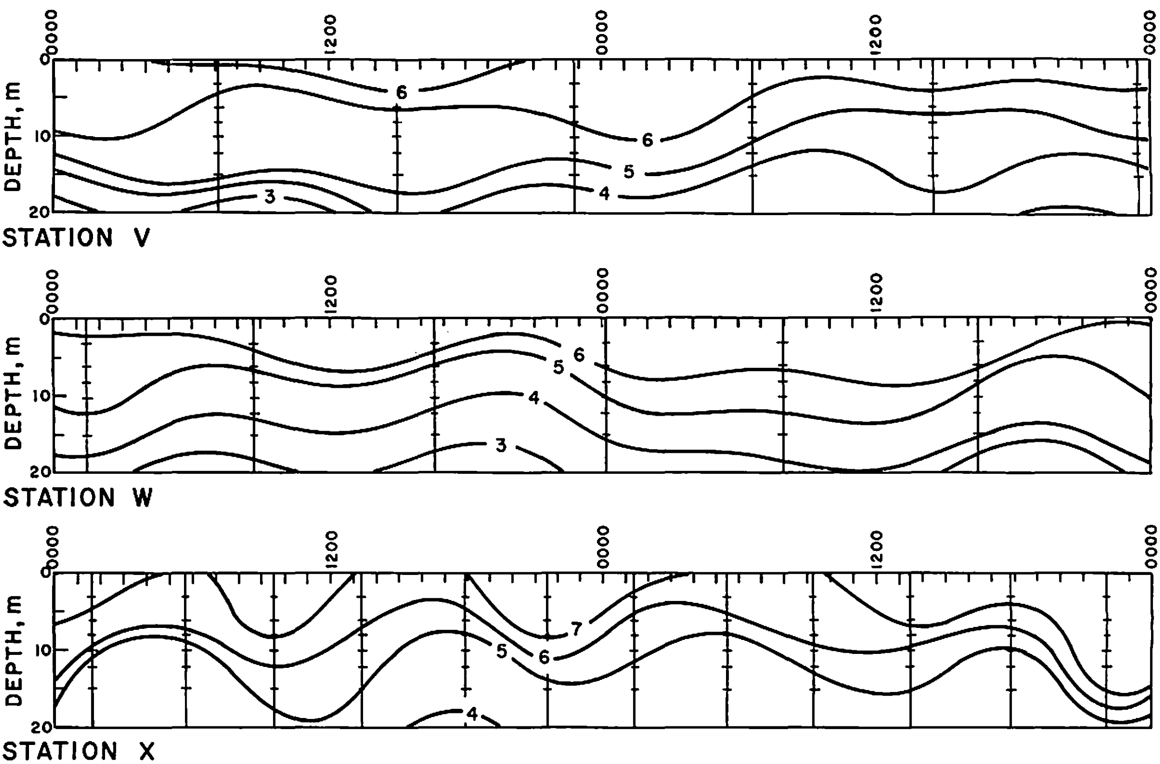

tinues to decrease between X and Z as it starts to increase between V and X. This causes a bulge in the isohaline surface at X and appears to be in response to the salt water wedge moving eastward inshore toward the channel entrance as the low salinity surface effluent moves back into the river estuary. At the half-tide mark (between low water and the next high water) the saltier water continues to move toward the estuary mouth and the surface becomes stationary along the VXZ line.

The motion of the tilted isohaline surface toward Z occurs over approximately a six-hour span bracketing high water. It appears to be steady except for initial and terminal accelerations. The advance of the surface

FIGURE 5. *Continued*

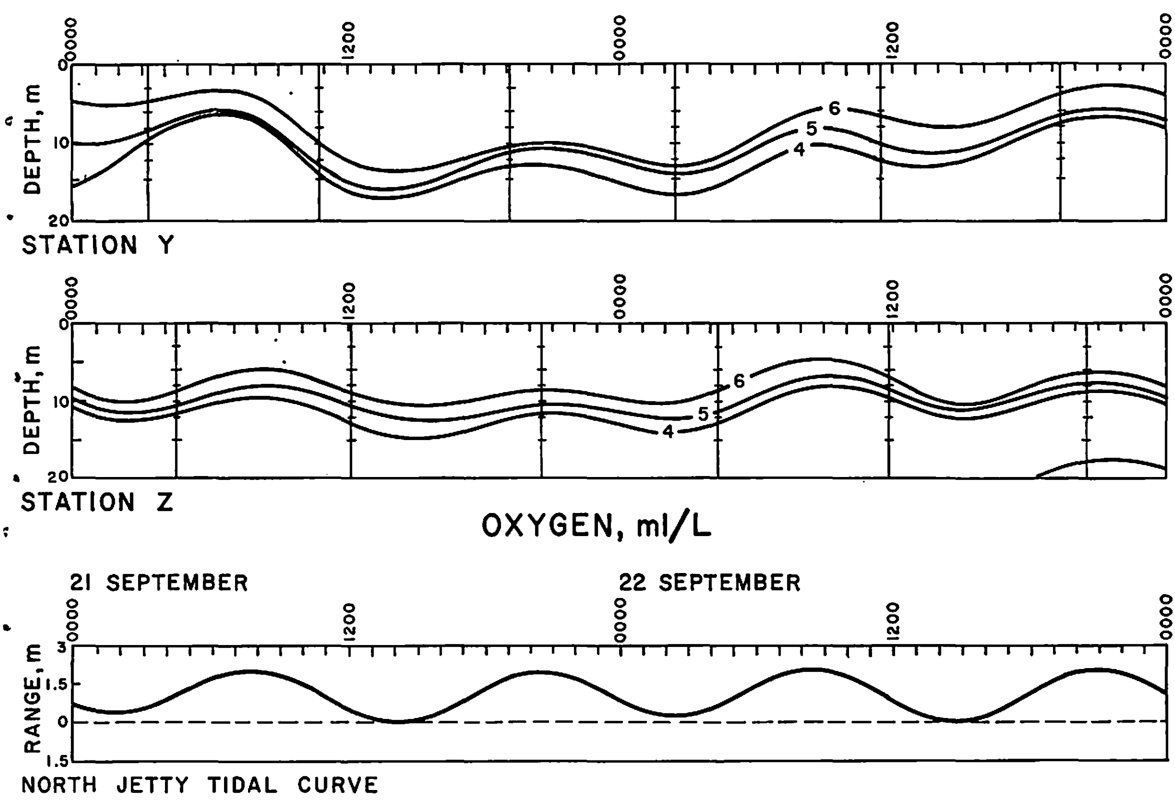

toward V, which occurs just before low water and ends shortly after it occupies a shorter span of time. These changes are consistent with the ebb and flood pattern in the river. On the falling tide the discharge of the tidal prism plus the discharge of the river enter into the grid area, while on the rising tide only the volume of the tidal prism flows into the river, opposing the outward river flow. Figs. 3-5 show that the river effluent appears at station X just after high water. The appearance of this river water requires the surface water at X to be in motion prior to high water to make room for the approaching dilute surface mass; therefore there is an early retreat of the surface waters toward Z and a deepening of the $31^{0}/_{00}$ surface at X as shown in Fig. 6. The space-time diagrams show that accelerations and changes in the isohaline surface appear more dramatic as the motion occurs over shorter periods of time. The oblique projection used in these diagrams distorts both the curves and the visual impression. Care should be taken that this distortion does not mislead the observer in estimating the acceleration.

The VXZ station line is oblique to the coast and approximately transverse to the axis of the usual summertime salinity distribution. However, the orientation of the river mouth and the horizontal distribution of observed data indicate that in summertime the effluent first moves outward on a line drawn from the river mouth toward station V, then moves southward toward X and Y. This injection of river water during the ebb stage causes a lateral motion of the edge of the dilute surface mass and produces the displacement of the tilted $31^{0}/_{00}$ surface toward Z; the surface returns to its initial position as the ebb ceases. This outward then southward flow is further apparent if one observes the change in slope of the $31^{0}/_{00}$ surface as the sloping surface starts moving from W toward Y immediately before high water. Midway between high water and the following low water the excursion stops and the effluent pool maintains a noticeably sharp lateral boundary. This lateral boundary is easily discerned where it produces the steep slope of the isohaline surface (dz/dx is large) and a sharp gradient of salinity. This boundary moves seaward, but not always past station X on the WXY line. Slightly after low water the surface loses its steep pitch at the edge of the effluent pool and it moves back toward W as the surface water retreats into the estuary.

Fig. 6 shows a definite repetition of the foregoing sequences. There was, however, a noticeable departure from the cyclic behavior between 0000 hr and 1400 hr on September 22. Prior to this period the winds were gentle and northwesterly; then the winds shifted becoming moderate and southerly, remaining so until the end of this period (Fig. 2). This wind shift displaced the effluent sufficiently north and east that the oscillation induced by the edge of the low salinity pool was not detected in the grid area. A calm period and a northwesterly flow again followed these southerly winds and the tide-related oscillations reappeared.

The tidal curve appropriate for the North Jetty as determined from the 1964 tide tables (U.S. Department of Commerce, 1963), and the hourly vectors of the rotating tidal current hodograph, determined at the Columbia River lightship (Marmer, 1926) and corrected to tide times at the North Jetty, are shown in Fig. 6. These current vectors (referenced to north at the tops of the figures) show the tidal velocity in absence of long-term currents, net river flow, and wind-driven currents. The oblique time-distance plots for the two station lines VXZ and WXY are also drawn with north at the top of the figure. The consistent orientation permits the current vectors to show the near-surface tidal motion with respect to the two station lines. It is now evident that the motion of the tilted $31^{0}/_{00}$ surface along the two station lines is in close agreement with the rotating tidal current, with the exception noted in the preceding paragraph.

CONCLUSIONS

Time studies of water characteristics over small areas undergoing rapid change are possible using a single survey ship provided rapid time-sequenced observations at fixed positions can be coupled with data taken less frequently from these and other fixed positions. The correlation of observations with time at key stations helps define the shapes of the curves of time-dependent variables between discrete observation points. Data from the region of the Columbia River mouth collected and used in this manner showed that the pool of river effluent, in the absence of strong winds, oscillates approximately in the directions indicated by the local tidal hodograph, but the pool can be displaced from its usual position by winds. The displacement by winds does not necessarily prohibit the pool from having tidal oscillation. The reason for the cessation of the oscillation observed in this instance is believed to be the movement of the oscillating boundary out of the field of observation. Lateral oscillations of the primary effluent pool near the mouth of the river are shown by and oriented in the direction of motion of the strong salinity gradients marking its edges. If the dimensions of this primary pool are either smaller than or about equal to those of the grid of the stations, the motion of its edges can be discerned provided they lie within the grid. If a large pool is monitored over a small grid, and its tidal excursion is of the same order of magnitude as the grid distances, the location of the grid of stations becomes critical and the edges may be missed altogether. The grid used in this study worked well in determining the movement of the boundaries of the effluent pool, which was relatively small owing to low river discharge in late summer.

The motion of the surface in response to the edge of the primary pool is a combination of bodily displacement of the pool without modification of the slope of the boundary and a changing of the boundary slope without lateral displacement of the mean position of the pool. The displacement of the pool is believed to be closely associated with the rotational tidal currents whereas the change in boundary slope seems to be controlled primarily by the hydraulic head of the river effluent and the amount of water discharged from the estuary.

ACKNOWLEDGMENTS

The authors wish to express their appreciation to Dr. C. A. Barnes for his critical reading of the manuscript. This work was supported by the Office of Naval Research, Contract Nonr-477(37), Project 083 012 and the Atomic Energy Commission, Contract AT(45-1)-1725 (Report no. RLO-1725-74).

REFERENCES

Budinger, T. F., L. K. Coachman, and C. A. Barnes. 1964. *Columbia River effluent in the northeast Pacific Ocean, 1961, 1962: selected aspects of physical oceanography*. Univ. Washington, Dep. Oceanog., Tech. Rep. No. 99. 78 p.

Cairns, J. L., and E. C. Lafond. 1966. Periodic motions of the seasonal thermocline along the southern California coast. *J. Geophys. Res. 71,* 3903-3915.

Marmer, H. A. 1926. *Costal currents along the Pacific Coast of the United States.* U.S. Dep. Com., Coast Geod. Surv., Spec. Pub. No. 121. 80 p.

Pattulo, J., and W. Denner. 1965. Processes affecting seawater characteristics along the Oregon coast. *Limnol. Oceanog. 10,* 443-450.

U.S. Department of Commerce, Coast and Geodetic Survey. 1963. *Tide tables, high and low water predictions, 1964, west coast of North and South America, including the Hawaiian Islands.* Washington, D.C. 224 p.

FIGURE 6. Depth of the 31‰ isosaline surface versus time along the two intersecting station lines, WXY and VXZ and the vectors, speed and direction, of the tidal current at the Columbia Lightship.

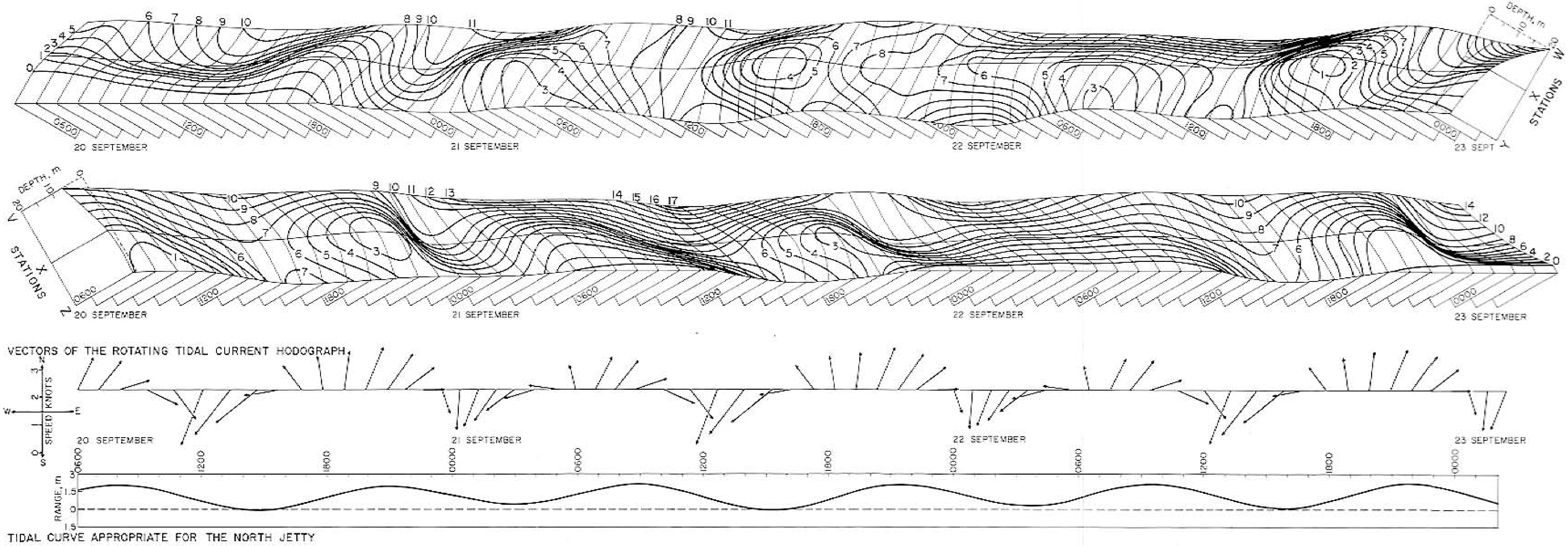

UNCLASSIFIED TECHNICAL REPORTS DISTRIBUTION LIST
FOR OCEANOGRAPHIC CONTRACTORS
OF THE OCEAN SCIENCE & TECHNOLOGY GROUP
OF THE OFFICE OF NAVAL RESEARCH
(Revised April 1967)

DEPARTMENT OF DEFENSE

Chief, Environmental Sciences Div.
Office of Director of Defense Research
and Engineering
Washington, D. C. 20301
1 Attn: Office, Assistant Director
(Research)

Navy

2 Office of Naval Research
Ocean Science & Technology Group
Department of the Navy
Washington, D. C. 20360
1 Attn: Surface & Amphibious Programs
(Code 463)
1 Attn: Undersea Programs (Code 466)
1 Attn: Field Projects (Code 418)
1 Attn: Geography Branch (Code 414)

1 Commanding Officer
Office of Naval Research Branch Office
495 Summer Street
Boston, Massachusetts 02210

1 Commanding Officer
Office of Naval Research Branch Office
219 South Dearborn Street
Chicago, Illinois 60604

1 Commanding Officer
Office of Naval Research Branch Office
1030 East Green Street
Pasadena, California 91101

5 Commanding Officer
Office of Naval Research Branch Office
Box 39, Fleet Post Office
New York, New York 09510

6 Director
Naval Research Laboratory
Washington, D. C. 20390
Attn: Code 5500

2 Commander
U. S. Naval Oceanographic Office
Washington, D. C. 20390
1 Attn: Code 1640 (Library)
1 Attn: Code 031
1 Attn: Code 70
1 Attn: Code 90

1 West Coast Support Group
U. S. Naval Oceanographic Office
c/o U. S. Navy Electronics Laboratory
San Diego, California 92152

1 U. S. Naval Oceanographic Office
Liaison Officer (Code 332)
Anti-Submarine Warfare Force
U. S. Atlantic Fleet
Norfolk, Virginia 23511

1 U. S. Naval Oceanogaphic Office
Liaison Officer
Anti-Submarine Warfare Force Pacific
Fleet Post Office
San Francisco, California 96610

1 Commander-in-Chief
Submarine Force Pacific Fleet
Fleet Post Office
San Francisco, California 96610

1 Commander-in-Chief
Pacific Fleet
Fleet Post Office
San Francisco, California 96610

1 Chief
Naval Ordnance Systems Command
Department of the Navy
Washington, D. C. 20360

1 Chief
Naval Air Systems Command
Department of the Navy
Washington, D. C. 20360
1 Attn: AIR 370E

1 Office of the U. S. Naval Weather
Service
Washington Navy Yard
Washington, D. C. 20390

1 Chief
Naval Facilities Engineering Command
Department of the Navy
Washington, D. C. 20390
1 Attn: Code 70

U. S. Navy Electronics Laboratory
San Diego, Califronia 92152
1 Attn: Code 3102
1 Attn: Code 3060C

1 Commanding Officer and Director
U. S. Naval Civil Engineering Labortory
Port Hueneme, California 93041

1 Commanding Officer
Pacific Missile Range
Pt. Mugu, Hueneme, California 93041

1 Commander, Naval Ordnance Laboratory
White Oak
Silver Spring, Maryland 20910

1 Commanding Officer
Naval Ordnance Test Station
China Lake, California 93557

1 Commanding Officer
Naval Radiological Defense Laboratory
San Francisco, California 94135

1 Commanding Officer
U.S. Naval Underwater Ordnance Station
Newport, Rhode Island 02840

1 Chief
Naval Ship Systems Command
Department of the Navy
Washington, D. C. 20360
1 Attn: Code 1622B

1 Officer-in-Charge
U. S. Navy Weather Research Facility
Naval Air Station, Bldg. R-48
Norfolk, Virginia 23511

1 Commanding Officer
U. S. Navy Air Development Center
Warminster, Pennsylvania 18974
1 Attn: NADC Library

1 U. S. Fleet Weather Central
Joint Typhoon Warning Center
COMNAVMARIANAS Box 12
San Francisco, California 94101

1 Superintendent
U. S. Naval Academy
Annapolis, Maryland 21402

2 Department of Meteorology & Oceanography
U. S. Naval Postgraduate School
Monterey, California 93940

1 Commanding Officer
U. S. Navy Mine Defense Laboratory
Panama City, Florida 32402

1 Commanding Officer
U. S. Naval Underwater Sound Laboratory
New London, Connecticut 06321

1 Officer-in-Charge
U. S. Fleet Numerical Weather Facility
U. S. Naval Postgraduate School
Monterey, California 93940

Air Force

1 Headquarters, Air Weather Service
(AWSS/TIPD)
U. S. Air Force
Scott Air Force Base, Illinois 62225

1 AFCRL (CRZF)
L. G. Hanscom Field
Bedford, Massachusetts 01730

Army

1 Coastal Engineering Research Center
Corps of Engineers
Department of the Army
Washington, D. C. 20310

1 Army Research Office
Office of the Chief of R&D
Department of the Army
Washington, D. C. 20310

1 U. S. Army Beach Erosion Board
5201 Little Falls Road, N. W.
Washington, D. C. 20016

1 Director
U. S. Army Engineers Waterways
Experiment Station
Vicksburg, Mississippi 49097
1 Attn: Research Center Library

OTHER GOVERNMENT AGENCIES

20 Defense Documentation Center
Cameron Station
Alexandria, Virginia 20305

2 National Research Council
2101 Constitution Avenue, N. W.
Washington, D. C. 20418
Attn: Committee on Undersea Warfare
Attn: Committee on Oceanography

1 Laboratory Director
California Current Resources Laboratory
Bureau of Commercial Fisheries
P. O. Box 271
La Jolla, California 92037

1 Director
Coast & Geodetic Survey - U.S. ESSA
Attn: Office of Hydrography & Oceanography
Washington Science Center
Rockville, Maryland 20852

1 Director
Atlantic Marine Center
Coast & Geodetic Survey - U.S. ESSA
439 West York Street
Norfolk, Virginia 23510

1 Director
Institute for Oceanography
U. S. ESSA
Gramax Building
Silver Spring, Maryland 20910

1 U. S. ESSA
Geophysical Sciences Library (AD 712)
Washington Science Center
Rockville, Maryland 20852

1 Commanding Officer
Coast Guard Oceanographic Unit
Bldg. 159, Navy Yard Annex
Washington, D. C. 20390

1 Chief, Office of Marine Geology &
Hydrology
U. S. Geological Survey
Menlo Park, California 94025

1 Director
Pacific Marine Center
Coast and Geodetic Survey - U.S. ESSA
1801 Fairview Avenue, East
Seattle, Washington 98102

1 Geological Division
Marine Geology Unit
U. S. Geological Survey
Washington, D. C. 20240

1 National Science Foundation
Office of Sea Grant Programs
1800 G Street, N. W.
Washington, D. C. 20550

1 Laboratory Director
Bureau of Commercial Fisheries
Biological Laboratory
450-B Jordon Hall
Stanford, California 94035

1 Bureau of Commercial Fisheries
U. S. Fish & Wildlife Service
P. O. Box 3830
Honolulu, Hawaii 96812

1 Laboratory Director
Biological Laboratory
Bureau of Commercial Fisheries
P. O. Box 3098, Fort Crockett
Galveston, Texas 77552

1 Laboratory Director
Biological Laboratory
Bureau of Commercial Fisheries
P. O. Box 1155
Juneau, Alaska 99801

1 Laboratory Director
Biological Laboratory
Bureau of Commercial Fisheries
P. O. Box 6
Woods Hole, Massachusetts 02543

1 Laboratory Director
Biological Laboratory
Bureau of Commercial Fisheries
P. O. Box 280
Brunswick, Georgia 31521

1 Laboratory Director
Tuna Resources Laboratory
Bureau of Commercial Fisheries
P. O. Box 271
La Jolla, California 92037

1 Bureau of Commercial Fisheries & Wildlife
U. S. Fish and Wildlife Service
Librarian
Sandy Hook Marine Laboratory
P. O. Box 428
Highlands, New Jersey 07732

1 Director
National Oceanographic Data Center
Washington, D. C. 20390

1 Laboratoy Director
Biological Laboratory
Bureau of Commercial Fisheries
#75 Virginia Beach Drive
Miami, Florida 33149

1 Director, Bureau of Commercial Fisheries
U.S. Fish & Wildlife Service
Department of the Interior
Washington, D. C. 20240

1 Bureau of Commercial Fisheries
Biological Laboratory, Oceanography
2725 Montlake Boulevard, East
Seattle, Washington 98102

1 Dr. Gene A. Rusnak
U. S. Geological Survey
Marine Geology & Hydrology
345 Middlefield Road
Menlo Park, California 94025

1 Assistant Director
Oceanography Museum of Natural History
Smithsonian Institution
Washington, D. C. 20560

1 Advanced Research Projects Agency
The Pentagon
Washington, D. C. 20310
Attn: Nuclear Test Detection Office

RESEARCH LABORATORIES

1 Document Library LO-206
Woods Hole Oceanographic Institution
Woods Hole, Massachusetts 02543

1 Director
Narragansett Marine Laboratory
University of Rhode Island
Kingston, Rhode Island 02881

1 Gulf Coast Research Laboratory
Ocean Springs, Mississippi 39564
Attn: Librarian

1 Chairman, Department of
Meteorology & Oceanography
New York University
New York, New York 10453

1 Director
Lamont Geological Observatory
Columbia University
Palisades, New York 10964

1 Director
Hudson Laboratories
145 Palisade Street
Dobbs Ferry, New York 10522

1 Great Lakes Research Division
Institute of Science & Technology
University of Michigan
Ann Arbor, Michigan 48105

1 Department of Physics
Northern Michigan University
Marquette, Michigan 49855

1 Director
Chesapeake Bay Institute
Johns Hopkins University
Baltimore, Maryland 21218

1 Director, Marine Laboratory
University of Miami
#1 Rickenbacker Causeway
Miami, Florida 33149

2 Head, Department of Oceanography &
Meteorology
Texas A&M University
College Station, Texas 77843

1 Director
Scripps Institution of Oceanography
La Jolla, California 92037

1 Allan Hancock Foundation
University Park
Los Angeles, California 90007

1 Head, Department of Oceanography
Oregon State University
Corvallis, Oregon 97331

1 Director, Arctic Research Laboratory
Pt. Barrow, Alaska 99723

1 Head, Department of Oceanography
University of Washington
Seattle, Washington 98105

1 Director
Institute of Marine Sciences
University of Alaska
College, Alaska 99735

1 Director
Bermuda Biological Station for Research
St. Georges, Bermuda

1 Director
Hawaiian Marine Laboratory
University of Hawaii
Honolulu, Hawaii 96825

1 President
Osservatorio Geofisico Sperimentale
Trieste, Italy

1 Department of Engineering
University of California
Berkeley, California 94720

1 Applied Physics Laboratory
University of Washington
1013 N. E. Fortieth Street
Seattle, Washington 98105

1 Physical Oceanographic Laboratory
Nova University
1786 S. E. Fifteenth Avenue
Fort Lauderdale, Florida 33316

1 Director
Ocean Research Institute
University of Tokyo
Tokyo, Japan

1 Marine Biological Association
of the United Kingdom
The Laboratory
Citadel Hill
Plymouth, England

1 Serials Department
University of Illinois Library
Urbana, Illinois 61801

1 New Zealand Oceanographic Institute
Department of Scientific and
Industrial Research
P. O. Box 8009
Wellington, New Zealand
Attn: Librarian

1 Director
Instituto Nacional de Oceanographia
Rivadavia 1917-R25
Buenos Aires, Argentina

1 Lieutenant Nestor C. L. Granelli
Head, Geophysics Branch
Montevideo 459, 4° "A"
Buenos Aires, Argentina

1 Oceanographische Forschungsantalt
der Bundeswehr
Lornsenstrasse 7
Kiel, Federal Republic of Germany

1 Underwater Warfare Division
of the Norwegian Defense Research
Establishment
Karljohansvera, Horten, Norway

1 Department of Geodesy & Geophysics
Columbia University
Cambridge, England

1 Institute of Oceanography
University of British Columbia
Vancouver, B. C., Canada

1 Department of the Geophysical Sciences
University of Chicago
Chicago, Illinois 60637

1 Coastal Engineering Laboratory
University of Florida
Gainesville, Florida 32601

1 Marine Science Center
Lehigh University
Bethlehem, Pennsylvania 18015

1 Institute of Geophysics
University of Hawaii
Honolulu, Hawaii 96825

1 Mr. J.A. Gast
Wildlife Building
Humboldt State College
Arcata, California 95521

1 Department of Geology & Geophysics
Massachusetts Institute of Technology
Cambridge, Massachusetts 02139

1 Division of Engineering and
Applied Physics
Harvard University
Cambridge, Massachusetts 02138

1 Department of Geology
Yale University
New Haven, Connecticut 06520

1 Westinghouse Electric Corporation
1625 K Street, N. W.
Washington, D. C. 20006